Title
Universal crossed molecular beams apparatus with synchtrotron photoionization mass spectrometric product detection

Permalink

Journal
Review of Scientific Instruments, 68(9)

Author
Yang, X.

Publication Date
1997-04-01

LBNL-40194
UC-401
Preprint

ERNEST ORLANDO LAWRENCE
BERKELEY NATIONAL LABORATORY

A Universal Crossed Molecular Beams Apparatus with Synchrotron Photoionization Mass Spectrometric Product Detection

X. Yang, D.A. Blank, J. Lin, A.G. Suits,
Y.T. Lee, and A.M. Wodtke
Chemical Sciences Division

April 1997
Submitted to
Review of Scientific Instruments

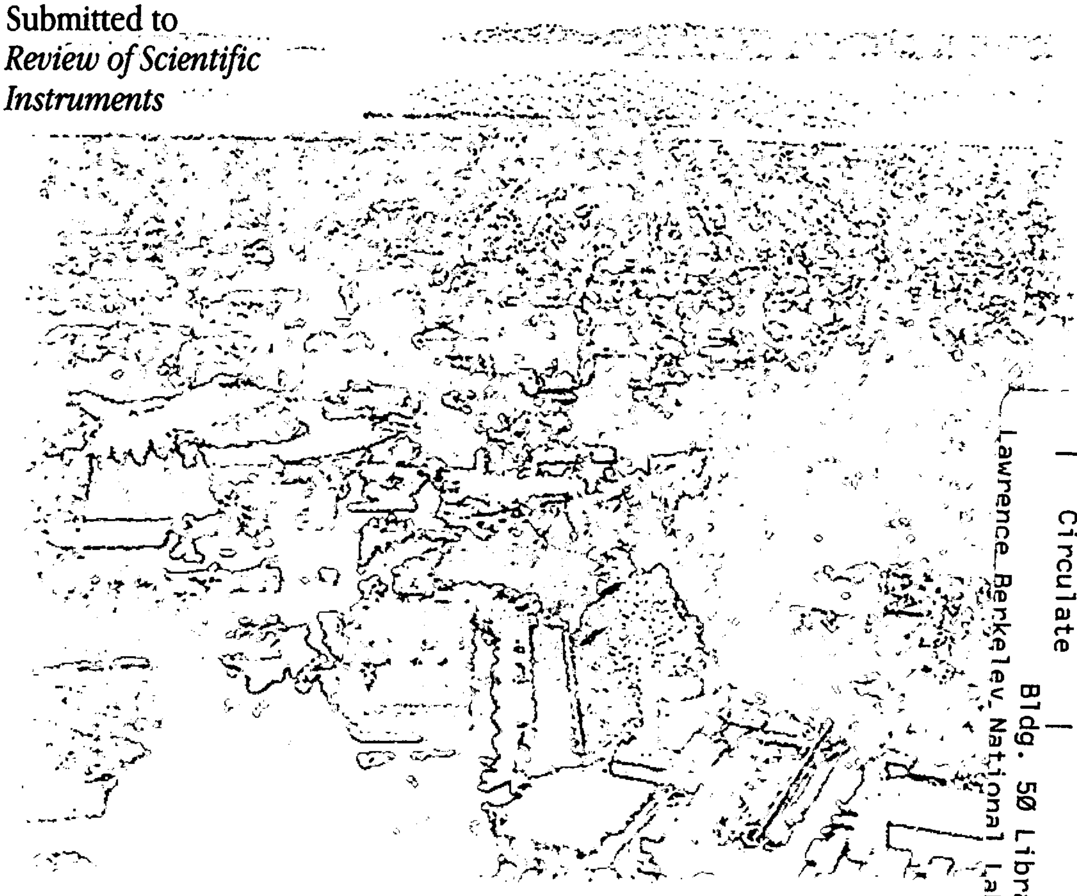

LBNL-40194
UC-401

A Universal Crossed Molecular Beams Apparatus with Synchrotron Photoionization Mass Spectrometric Product Detection

X. Yang,[1] D.A. Blank,[2] J. Lin,[1] A.G. Suits,[2] Y.T. Lee,[1] and A.M. Wodtke[3]

[1]Institute of Atomic and Molecular Sciences
Academia Sinica
P.O. Box 23-166
Taipei, Taiwan, ROC

[2]Department of Chemistry
University of California, Berkeley
and
Chemical Sciences Division
Ernest Orlando Lawrence Berkeley National Laboratory
University of California
Berkeley, California 94720

[3]Department of Chemistry
University of California
Santa Barbara, CA 93106

April 1997

This work was supported by the Director, Office of Energy Research, Office of Basic Energy Sciences, Chemical Sciences Division, of the U.S. Department of Energy under Contract No. DE-AC03-76SF00098.

A Universal Crossed Molecular Beams Apparatus with Synchrotron Photo-ionization Mass Spectrometric Product Detection,

X. Yang[1], D. A. Blank[2], J. Lin[1], A. G. Suits[2] and Y. T. Lee[1] and A. M. Wodtke[3]

Abstract: Vacuum ultraviolet radiation was generated from an undulator at the Advanced Light Source Synchrotron facility and used for photo-ionization detection of reaction products in a new universal crossed molecular beams machine. A description of the machine and its performance is presented. Initial experiments on the photodissociation of Methylamine (CH_3NH_2), Ozone (O_3) , Oxalyl chloride ($(OCCl)_2$) as well as the reactive scattering of Cl with C_3H_8 show many of the advantages of photo-ionization in comparison to electron impact ionization, which has been exclusively used in such instruments in the past. "Momentum matching" of reaction products is much more easily accomplished than in electron impact studies due to the complete suppression of dissociative ionization. The tunability of the VUV radiation can be used to suppress background from residual gases especially when it is desired to detect free radical reaction products. Even when the tunability cannot be used to suppress background, the fact that little heat is generated by the ionizing beam allows background to be substantially suppressed by cryogenic pumping. The energy resolution of the apparatus is comparable to instruments that have previously been designed with electron impact ionization which have more than twice as a long of a flight path. This new instrument provides outstanding performance for fundamental studies of chemical dynamics.

---

[1] Institute of Atomic and Molecular Sciences, Academia Sinica, P.O. Box 23-166, Taipei, Taiwan, ROC

[2] Chemical Sciences Division, Lawrence Berkeley National Laboratory and Department of Chemistry, University of California, Berkeley CA 94720

[3] Department of Chemistry, University of California, Santa Barbara, CA 93106

1. Introduction

The development of universal crossed-molecular-beams instruments, originally reported in this journal *(1)*, has aided the improvement of our understanding of bimolecular and unimolecular chemical reactions. Copious and fundamental information has been derived on: primary reaction mechanisms, product angular distributions, partitioning of reaction exothermicity between product internal and translational energy, as well as the dependence of reaction cross-section on collision energy, impact parameter and reactant orientation *(2)*. Central to the usefulness of such an apparatus is its ability to deliver time-of-flight (TOF) spectra of all chemical or photochemical reaction products as a function of laboratory recoil angle. Such experimental data can be analyzed to yield the center-of-mass frame differential scattering cross-section, or "product flux map", a fundamental quantity that reflects the interatomic forces governing the reaction. Up until now, all universal crossed-molecular-beams instruments have relied on electron impact ionization (EI) mass spectrometry to provide sensitive, time-resolved product detection. Using EI, a product flux smaller than 10^4 molecules cm^{-2} s^{-1} (0.1 molecule cm^{-3} at a velocity of 10^5 cm/s) can be detected with a time response better than 10^{-6} s.

Despite its success, EI possesses several significant disadvantages. First and foremost, EI often results in dissociative ionization of the neutral reaction product. In this case, the reaction product is not detected with a mass-to-charge ratio (m/z) equal to the mass of the neutral. This can greatly complicate the identification of reaction products particularly when several reaction channels occur simultaneously. Second, EI, which requires a hot filament ($T_{filament} = 2000\text{-}3000$ K), increases the background partial pressure of many species present in the detector chamber increasing the background upon which the signal must be detected. Third, EI's universality, its chief advantage, is also one of its biggest disadvantages. As an example, it is nearly impossible to construct a high vacuum chamber out of stainless steel and lower the CO partial pressure below 10^{-11} torr. Detection of any ion with m/z = 28, is difficult at best. Indeed detection of ions with m/z = 29 or 27 is likely to be impossible. Similar arguments hold for detection of products at m/z

= 1, 2, 15, 16 18 and 44, due to trace backgrounds of H_2, CH_4 and CO_2. In a similar vein, the operation of the molecular beam sources gives rise to an increase in the partial pressures of molecules which, when dissociatively ionized, can produce background at the m/z-value of the detected product. Finally, EI's sensitivity and time resolution are limited by space charge effects. At the highest electron currents, the ionizing electron beam "repels itself", increasing its volume and lowering the electron flux available for product detection. Furthermore, ionization of products to positive ions at the highest electron flux makes ion extraction to the mass spectrometer impossible on the μs time-scale, since the electron cloud shields the positive ions from the extraction voltages.

Photo-ionization (PI) overcomes all of these problems. First, when the wavelength is tuned below the dissociative ionization potential of a molecule it is a "soft" (non-dissociative) ionization method. Reaction products of mass, m, will be detected as ions with mass to charge ratio of m. Second, PI does not generate significant amounts of heat (~20 mW in comparison to 20 W for electron impact). Thus it can be employed in concert with cryogenic pumping methods. In this way the ionization region itself may be cooled with Liquid Helium, further suppressing the partial pressure of many background gases. Third, PI can be universal *and* selective, since the wavelength of the light may be tuned. For example, the wavelength tunability can be used to suppress background due to the most common residual gases, CO (I.P. = 14.01 eV), CH_4 (I.P. = 12.51 eV), H_2O (I.P. = 12.61 eV), H_2 (I.P. = 15.43 eV). The tunability may also be employed to detect products with different amounts of internal energy since the ionization threshold of a molecule depends on its energy content. Finally, PI is not subject to space charge effects, since photons are not charged. Therefore, light can be focussed much more tightly than can electrons. Consequently, one can produce very small ionization volumes which provide high time resolution for TOF measurements. Furthermore, there is no fundamental physical limit to the ionization efficiency. As greater and greater VUV flux becomes available, higher and higher detection sensitivity can be achieved.

Despite its clear desirability, vacuum ultraviolet (VUV) PI has never been implemented in a universal crossed molecular beams machine. Table top VUV light sources (which rely on non-linear frequency conversion of pulsed laser light) cannot offer the ~10^{16} photons/s needed for crossed-molecular beams experiments. However, the Advanced Light Source (ALS), a recently developed third generation synchrotron radiation source at the Lawrence Berkeley National Laboratory is suitable for this application.

In this paper we describe the design and performance of a new crossed molecular beams machine which utilizes the ALS as a source of ionizing radiation. With this machine we have succeeded in demonstrating all of the advantages mentioned in this introduction.

2. Apparatus Description

a. Design criteria

The design criteria for a crossed molecular beams machine have been previously discussed *(1)*. The apparatus must contain two collimated supersonic molecular beams which cross one another at a distance from the nozzles such that the probability is negligible for a molecule in the first beam to suffer more than one collision with molecules in the second beam. Furthermore, the probability for collisions between molecules in different molecular beams must be much larger than the probability for intrabeam collisions as well as collisions of molecules in one of the molecular beams with background gas. In order to ensure these "single collision conditions", the density of the molecular beams should in the rage of 10^{11-12} molecules cm^{-3} at the point where the molecular beams cross. For continuous beams, this requires both beam sources be separately housed with their own differential pumping systems. In this way the source chamber's operating pressure of ~10^{-3} torr ($3x10^{13}$ molecules cm^{-3}) may be reduced by a single differential pumping chamber to lower than 10^{-7} torr ($3x10^{9}$ molecules cm^{-3}) in the interaction chamber. The contrast ratio between the beam and background densities in the interaction chamber is maintained above 100 by this approach.

Reaction products are formed in the beam crossing volume with a typical density of ~10^{7} molecules

cm^{-3} and are scattered into a finite angular distribution. A small fraction of these are scattered into the solid angle subtended by the mass spectrometric detector. The partial pressure of the reaction products at the ionizer of the detector can be as low as 10^{-15} torr (30 molecules cm^{-3}). In order to detect this small sample, special steps must be taken to reduce the background partial pressure of residual gasses as well as gasses that enter the detector due to the operation of the molecular beams. This requires that the detector be extensively differentially pumped and techniques of ultrahigh vacuum be employed. The beam sources and the detector must also rotate with respect to one another in order that the complete product flux map be obtained.

The use of synchrotron radiation imposes additional design restrictions, associated with the strict vacuum requirements necessary for successful synchrotron operation and the fact that the ionizing light beam must remain fixed in space. The 0.4 Ampere relativistic electron beam producing synchrotron radiation at the ALS requires exceptionally clean vacuum conditions. The consequences of contaminating the synchrotron ring due to accidental vacuum loss in one of the end-stations prohibits the use of diffusion pumps, commonly used with molecular beam machines. In addition, since the ionizer must be fixed in space, the beam *sources* must rotate in order to sample different recoil angles. Such a design has been previously developed for a single molecular beam using a fixed diffusion pump *(3)* but never have two rotating beam sources been constructed.

b. Overview of the machine and description of the Vacuum system

One of the most important considerations in the design of an instrument such as this one is the differential pumping system which allows for production of intense continuous or pulsed molecular beams in one part of the machine operating at pressures up to 10^{-2} torr, while maintaining ultra-high vacuum ($p_{tot} < 5 \times 10^{-11}$ torr) for a mass-spectrometric detector in another part of the machine. We have chosen magnetically levitated turbo molecular pumps to fulfill the design requirements. Unlike diffusion pumps these pumps may be mounted in any orientation and move with the rotating sources. Furthermore, since they have no pumping or lubricating fluid, the entire instrument may be made oil-free. Fast-trip gate valves together with differential pumping stages located between the synchrotron ring and the end-station prevent vacuum loss in the molecular beam machine from affecting the synchrotron ring.

An overview schematic of the machine is shown in fig. 1. Two molecular beam sources, fixed at a 90^0 crossing angle, rotate together with respect to the detection axis. The molecular beam source assembly can be rotated from -20^0 to 110^0 degrees so that both beams may point into the detector for beam diagnostic purposes. Each of the two molecular beam sources consist of two separately pumped chambers, a source chamber and a differential pumping chamber. These four chambers are pumped, respectively by two source pumps (high-throughput chemically resistant 2000 ℓ/s turbo-molecular pumps -- Seiko Seiki STPH2000C) and two differential pumps (a 250 ℓ/s Osaka TG250M and a 400 ℓ/s turbo-molecular pump -- Seiko Seiki STP400). All four pumps are magnetically levitated and can be held at any orientation. Three of the four pumps are attached directly to the rotating source assembly and move when the source is rotated. One of the differential pumps is attached to a fixed "buffer chamber" which is sealed by a rotating vacuum seal to the source chamber. During operation, the source chamber's pressures are typically 10^{-3} torr and the differential pumping chamber's pressures are 10^{-5} torr.

The main interaction chamber is a large stainless steel cube, evacuated by a 2000 ℓ/s turbo molecular pump (Seiko Seiki STP2000C) backed by an oil free scroll pump (Edwards ESDP-30), which holds the rotating source assembly. The main chamber is continuously cryo-pumped by large liquid nitrogen cooled panels which line the walls of the chamber. The main chamber pressure is typically 10^{-8} torr during operation.

A large square port on the interaction chamber is keyed to align the detector to the rotation axis of the sources and the crossing volume of the molecular beams. The detector has four differentially pumped chambers. The first two (labeled I and II in fig. 1) are pumped by 300 ℓ/s turbo molecular pumps (Seiko Seiki STP300) and reduce the main chamber pressure effusing into the detector to $\sim 10^{-9}$

and 10^{-10} torr, respectively. Region III is a dual walled liquid nitrogen dewar, pumped by a 600 ℓ/s turbo molecular pump (Seiko Seiki STP600) housing an electron impact ionizer, a cryo-cooled region for PI and ion optics to transport the ions to region IV. The PI region is housed within a liquid Helium cooled shroud, whose temperature can be reduced to as low as 25 K. The ultimate pressure of region III is lower than 1.5×10^{-11} torr, which was the typical operating pressure in region III.

Region IV holds the Quadrupole (Extrel) mass spectrometer and standard Daly ion counter *(4)* and is pumped by a 300 ℓ/s magnetically levitated turbo molecular pump (Seiko Seiki STP300). All four turbo pumps on the detector are backed up by a 250 ℓ/s magnetically levitated turbo pump (Osaka TH-250MC), which is then backed up by an oil free scroll pump.

Despite this extensive pumping scheme, molecules which pass directly through the detector's differential pumping apertures along a line connecting the beam crossing volume and the ionization volume are immune to differential pumping and limit the lower level of the background in many experiments. Because the mean free path in the interaction chamber is of kilometer length, these "direct-through" molecules must *desorb* from surfaces which lie in the detector's viewing window, behind the beam crossing volume. To eliminate these molecules, a cryogenically cooled Copper plate is placed behind the molecular beam crossing volume and within the detector viewing window. When cooled to @30K little that adsorbs on this Copper plate can desorb into the detector.

c. *Details of the Rotating Source, Main and Detector Chambers*

The dual molecular beam rotating source assembly was one of the most complex parts of the machine to design. Fig. 2a and b are 3-D renderings of the rotating source assembly. Fig. 3a and b show mechanical drawings of the top view and a section through the source chamber as indicated. The entire chamber is welded from stainless steel and precision machined to tolerances of 0.002" by Huntington for all surface relevant to alignment of the experiment. The two large ports (12" CF flanges) on the "roof" of the source assembly are used to evacuate the source chambers themselves. The smaller circular port (8" CF flange) allows the differential pumping region of one of the beam sources to be evacuated.

Fig. 4 shows a mechanical drawing of the main chamber. The main chamber actually consists of two chambers: the interaction chamber and the buffer chamber for the second differential pumping chamber mentioned above. The 30" diameter opening is fit with three TEC rings (Carbon impregnated Teflon) and a rotating circular bearing (Kaydon). The space between the TEC-rings is evacuated by a small mechanical pump (Edwards E2M5). The dividing wall between the interaction and buffer chamber is also fit with a single-TEC ring seal and a rotating circular bearing. Inspection of sections A-A in figures 3 and 4 reveals that the rotating source assembly can be inserted into the main chamber. There is insufficient room to mount four large turbo molecular pumps on the roof of the source. So, the 8" CF flange on the buffer chamber (fig. 4. Section A-A) holds the fourth turbo molecular pump used to evacuate the differential pumping region of the second molecular beam source. This can be most easily seen in fig. 3 section A-A.

This design allows the molecular beam sources to be rotated about an axis containing the crossing point of the two molecular beams. Note that the rotation axis of the source provides a line of sight through the machine. This can be used to pass a laser beam or the VUV synchrotron beam for photochemistry experiments.

The main chamber has two large rectangular ports (as can be seen more clearly in the 3-D rendering of fig. 5). One of these is used to align the detector to the rotation axis of the source. The second is used for access to the interaction chamber and to the source chambers. Three long thin tubes parallel to the rotation axis are located 4, 6, and 10 inches away from the rotation axis and allow for entry of the VUV synchrotron radiation. The entire machine may be translated (after venting to atmosphere) along precision case-hardened stainless steel rails to allow for entry of the VUV light at either of these three locations or along the axis of rotation. The detector is shown inserted into the large rectangular port of the main chamber in fig. 1. Three views of the first two differential pumping chambers are also shown in fig. 6. Under normal operation, the PI volume is located 6" from the rotation axis of the source. In this arrangement the 2" CF flange shown in figure 6 section B-B connects to one of the synchrotron entry ports of the main chamber . A spacer may be inserted between the detector and the main chamber to increase the distance between the rotation axis and the PI volume to 10". For bake out, the detector can be removed entirely from the main chamber maintaining high vacuum.

d. The synchrotron radiation source and gas filter

The Advanced Light Source (ALS) is one of the first low emittance, third generation synchrotron radiation facilities available *(5)*. The design of the ALS is optimized for insertion devices (e.g. undulators and wigglers) which produce tunable VUV to soft X-ray radiation with much higher photon flux than bending magnets. These insertion devices, in particular undulators, offer the world's brightest sources of VUV light with a large duty factor. The raw undulator output is greater than 10^{16} photons/s with a bandwidth $\Delta\nu/\nu$ of 0.022. The undulator used for these experiments was 4.5 m in length and had 45 10-cm periods. The magnetic field of the undulator was 0.76 Tesla and was used with a 0.4 A beam of 1.5 GeV electrons. The K-value of the undulator was 7.1 at 150 nm. With such a high-K value which is required to efficiently produce VUV light at energies as low as 5 eV, substantial radiant power is emitted in the undulator's harmonics. For use in crossed molecular beams experiments these are undesirable, since they lead to dissociative ionization. Special measures must be taken to reduce the intensity of the harmonics. Fortunately, losses on the mirrors needed to guide the undulator output to the crossed molecular beams machine strongly attenuate the contribution from harmonics above 100 eV, and virtually eliminate everything higher than 500 eV, while at the same time directing and focusing the beam as desired.

One drawback of thin film filters and mirrors is a transmission gap ranging from the lithium fluoride cutoff at 11 eV to about 35 eV. For soft PI, this region is of considerable importance, since the third harmonic dominates the spectrum of the undulator harmonics and 11-12 eV will be frequently used for the fundamental. These considerations prompted us to develop a windowless harmonic filter employing rare gas (argon or neon) as the filter medium with differential pumping serving to preserve the beamline vacuum. The design characteristics of this device and its performance have been measured using a Transmission Grating Spectrometer and have been recently reported *(6-8)*. For all intents and purposes the higher harmonics are completely removed by the gas filter.

3. Performance of the apparatus: Preliminary Results

The machine is designed for two different kinds of experiments, which are presented here. First, a molecular beam may be crossed with the output of a pulsed laser which enters the machine along the rotation axis of the source assembly. The photofragments' arrival time distribution at the detector is then measured at a number of laboratory recoil angles. Second, two crossed molecular beams produce chemical reaction products. The products lab frame angular distribution can be obtained by measuring the signal intensity at different recoil angles. Alternatively, a slotted chopping wheel can be used to obtain the velocity distribution of the reaction products. In both of these experiments the center-of-mass frame velocity distribution of the products is derived using standard forward convolution methods.

a. Photodissociation of Methylamine at 193 nm

In order to help evaluate the performance of this instrument, a molecular beam of methylamine (5% CH_3NH_2 seeded in He) was crossed with the output of an Argon Fluoride excimer laser operating at 100 Hz, producing 10 mj/pulse of light at 193 nm. Photodissociation of methylamine at 222 nm has been previously studied using EI *(9)*. Evidence for a minor photodissociation channel was found in that work.

$$CH_3NH_2 \quad \rightarrow \quad CH_3 + NH_2 \qquad \text{R-1} \quad (1\%)$$

Detection of the products of this reaction is a "worst-case" example of the kind of problem frequently encountered with universal crossed-molecular beams machines. CH_3 radical exhibits a major peak in its mass spectrum at m/z = 15 (CH_3^+). NH_2 radical can be detected at m/z = 16 (NH_2^+). Painfully, the EI mass spectrum of CH_4, an important residual gas in most mass spectrometers has two peaks of near equal abundance, CH_4^+ (m/z =16) and CH_3^+ (m/z = 15) . Indeed in the electron impact work, detection of NH_2 was impossible since , "... high background obscured the extremely weak signal at m/z = 16..." *(9)*. In addition to residual Methane in the detector, the operation of the methylamine molecular beam causes the partial pressure of this species to rise significantly in the detector. The EI mass spectrum of this species has major peaks at m/z = 31-27 and 15. In order to identify reaction R-1 unambiguously, one needs to record TOF spectra of CH_3 and NH_2. This data can then be used to derive the center-of-mass translational energy distribution for this reaction. If this analysis is successful, the two fragments are said to be "momentum matched". Such terminology is used to indicate the fact that conservation of momentum and energy allows the CH_3 TOF spectrum to be determined from the NH_2 TOF and *vice versa*. If this analysis fails, it means that the two observed fragments are formed in different dissociation processes.

This process of "momentum matching" the TOF spectra is crucial to the analysis of data obtained with EI, since dissociative ionization of larger neutral fragments can complicate the data. For example in the electron impact study mentioned above the m/z = 15 TOF spectrum has contributions from CH_3, NH_2, CH_3NH and CH_2NH_2 *(9)*, the last two of which were formed from other photodissociation pathways:

$CH_3NH_2 \rightarrow CH_3NH + H$

H-Atom loss channels (99%)

$\rightarrow CH_2NH_2 + H$

Inspection of the thresholds of the ionization events which are responsible for production of ions at m/z = 15 and 16 shows how these problems can be solved with the new instrument. Here the processes resulting in desired signal are indicated in bold font.

$CH_4 \rightarrow CH_3^+ + H + e^-$ 14.3_5 eV

$CH_3NH_2 \rightarrow CH_3^+ + NH_2 + e^-$ 13.5_2 eV

$CH_4 \rightarrow CH_4^+ + e^-$ 12.51 eV

$\mathbf{NH_2 \rightarrow NH_2^+ + e^-}$ **11.14 eV**

$\mathbf{CH_3 \rightarrow CH_3^+ + e^-}$ **9.84 eV**

By tuning the wavelength of the light between 12.51 and 11.14 eV the background can be completely suppressed. In practice, because the cross-section of each process is small near threshold, one can increase the PI energy to 13 eV in this example, where it was found that one obtained the maximum sensitivity for PI of products while still suppressing background.

Figure 7 shows the TOF spectra for m/z=15 and 16 at $\theta=25^0$ obtained from 4 x 10^5 laser shots. The solid lines passing through the data are the result of the forward convolution analysis used routinely for such experiments. The good fit to each TOF spectrum indicates that the products are momentum matched and that these TOF spectra have no contribution from other photodissociation pathways. The H-atom loss channels could however, be easily detected by adjusting the quadrupole mass spectrometer to observe m/z =30 and was found to be a much stronger signal, confirming that it is the dominant reaction pathway at 193 as well as 222 nm.

This example demonstrates the consequences of suppressing dissociative ionization using the wavelength tunability of the undulator. Clearly, one can suppress background from residual gas yielding in this case high signal-to-noise data at m/z = 16. Furthermore dissociative ionization of larger molecules, both dissociation parents and daughters have been suppressed, greatly simplifying the momentum matching procedure.

b. Photodissociation of Ozone at 248 nm

Experiments investigating the necessity of harmonic suppression and kinetic energy resolution of the new machine have also been carried out. Specifically, a molecular beam of 5% O_3 seeded in Argon was prepared and crossed with the output of a KrF laser emitting 20 ns pulses of 248 nm light containing 200 mJ of energy at 100 Hz. For this work a 4.5 m undulator was used with 56 8-cm periods and a value for K=7.9. The storage ring contained 1.5 GeV electrons. The entire unfiltered output was directed to the machine and the Argon gas filter was evacuated. The fundamental of the undulator was tuned to 18 eV, with a 1.9% bandwidth.

Figure 3 shows the TOF spectra obtained for m/z = 32 and 16 recorded after 200,000 shots. Please note the differing time scales of the two TOF spectra. Again, there is no evidence of the dissociative ionization of O_2 contaminating the m/z=16 TOF spectrum despite the lack of harmonic suppression. In contrast to recent studies using EI, where ozone was photodissociated at 193 nm, extensive dissociative ionization was observed and complicates the analysis in that work *(10)*.

These TOF spectra also give a measure of the energy resolution of the instrument. The individual peaks in the TOF spectra (labeled 0, 1, 2, 3 and 4) can be assigned to the 5 lowest vibrational states of $O_2(a^1\Delta)$ formed in the dominant dissociation channel:

$$O_3 \rightarrow O_2(a^1\Delta, v=0\text{-}4) + O(^1D_2).$$

Similar vibrationally resolved TOF spectra have been previously reported for photolysis of ozone at 266 nm using EI *(11)*. The energy resolution of that experiment was similar to this work. But this instrument uses a 15 cm flight path whereas the EI work required a 34 cm flight path to obtain vibrational resolution. Since the VUV may be tightly focussed due to the absence of space charge problems, the uncertainty in the flight path ($\Delta\ell/\ell$) is actually better in this machine ($\Delta\ell/\ell = 0.02$) than for the instrument used in reference *(11)* ($\Delta\ell/\ell = 0.03$). This points out an important feature of the new machine. High resolution TOF spectra may be obtained with a flight path that is more the a factor of two shorter. Since the product density drops with the square of the distance from their point of creation, the number density of the products in the new machine at the point of detection is 5.14 times larger than in reference *(11)*.

c. *Photodissociation of Oxalyl chloride*

As mentioned above, the synchrotron radiation generates very little heat in the detector allowing the use of cryogenic cooling around the PI region. In order to investigate the usefulness of this design concept we have obtained data on the photodissociation of oxalyl chloride, $(ClCO)_2$. The photochemistry of this molecule has been recently investigated and found to exhibit primary, secondary and tertiary dissociation chemistry at a photolysis wavelength of 230 nm *(12)*:

$$\begin{aligned} \text{Cl-CO-CO-Cl} &\rightarrow \text{Cl} + \text{Cl-CO-CO}\cdot, \\ \text{Cl-CO-CO}\cdot &\rightarrow \text{CO} + \text{COCl}, \\ \text{COCl} &\rightarrow \text{CO} + \text{Cl}, \end{aligned}$$

resulting in Cl and CO products. Cl-atoms ($m/z = 35$ and 37) are typically among the easiest of chemical fragments to be detected in a universal crossed molecular beams machine, since there is little source of background at these values of the mass to charge ratio.

The background at $m/z = 28$ is normally $10^{5\text{-}6}$ Hz in a conventional EI apparatus. As a result detection of CO reaction products at m/z = 28 is typically impossible or at least very difficult. In these experiments the output of the ALS was tuned to 14.8 eV, where ~35 mW of VUV radiation was obtained. The gas filter was used to suppress undulator harmonics. A continuous molecular beam 3-4% oxalyl chloride in He was formed by expansion through a 0.010" diameter orifice. With the PI region cooled to ~25K, the detector pressure was 1.5×10^{-11} torr with the molecular beam running. The background count rate at m/z = 28 was measured to be 4000 Hz when the source was rotated 20° away from the detection axis. This is an improvement in the background level for CO of between a factor of 100 and 1000.

Unlike the example of methylamine, the tunability of the synchrotron is not of much use for suppression of background, since one of the products of interest is an abundant residual gases in the detector. Fig. 9 shows a comparison of the Cl and CO TOF spectra obtained for the photoproducts of oxalyl chloride. The signal-to-noise in the two TOF spectra is comparable. Remarkably, experiments at m/z = 28 are not substantially more difficult than those at m/z = 35-37. This remarkable result opens up a large are of research into the photochemistry of Carbonyl containing compounds and areas of bimolecular reactions related to CO/CO_2 conversion.

d. Reactive scattering of $Cl + C_3H_8$

In order to evaluate the performance of the instrument in reactive scattering experiments, we have undertaken preliminary studies of the reaction

$$\mathrm{Cl} \quad + \quad \mathrm{C_3H_8} \qquad\qquad \mathrm{HCl} \quad + \quad \mathrm{C_3H_7}.$$

A continuous molecular beam of Cl-atoms was produced by pyrolysis of a 6% Cl_2 in He mixture in a heated graphite nozzle. This molecular beam had a peak velocity of 2800 ± 300 m/s. The propane beam was formed by expanding a 17% mixture of propane in Helium through a 0.010" diameter stainless steel orifice. The peak velocity of this beam was 1080 ± 100 m/s. The arrival time distribution of the reaction products was obtained using cross-correlation time-of-flight methods. Detection of the propyl radical, C_3H_7, was accomplished with PI using the output of the U-10 undulator tuned to 9.5 eV. In addition to the Argon gas filter, a MgF_2 window was used as an 11.2 eV cut-off filter.

The Newton diagram in fig. 10 reveals the relationship of the various velocity vectors important to this experiment. In this figure laboratory frame vectors are indicated with "v's" while center-of-mass frame vector are indicated with "u's". $\mathbf{v}_{CM}$ is the velocity vector of the center-of-mass of the collision system. The center-of-mass frame vector, **u**, and laboratory frame vector, **v**, are related by the vector equation $\mathbf{u} + \mathbf{v}_{CM} = \mathbf{v}$. The peak velocities of the Cl and C_3H_8 beams are labels $\mathbf{v}_{Cl}$ and $\mathbf{v}_{Propane}$, respectively. A TOF spectrum shown in fig. 10 results from products detected along the direction of the vector, $\mathbf{v}_{mp}$. Products formed with the most probable velocity in the center-of-mass frame, $\mathbf{u}_{mp}$, may be scattered anywhere on the circle touched by the tip of this vector. Products formed with the maximum velocity in the center-of-mass frame may be scattered anywhere on the circle touched by the tip of the vector $\mathbf{u}_{max}$. These kinematic conditions suggest that the propyl radical can be scattered into a wide range of angles in the laboratory frame meaning that only a very small fraction of the reactive flux can enter the detector at a give scattering angle. Indeed, the angular distribution of the propyl radical is broad with significant product flux in the forward and backward hemispheres and substantial signal was observed from -10° to 100°.

This reaction presents some of the most difficult problems that arise in reactive scattering experiments. H-atom transfer reactions such as this one are particularly difficult to study in crossed molecular beams experiments, due to the fact that the product mass is only removed from that of one of the reactants by one atomic mass unit. This presents two difficulties. First, if one want to detect $C_3H_7^+$ in the presence of large quantities of C_3H_8 or HCl^+ in the presence of large quantities of Cl, the mass resolution of the quadrupole must be substantially increased to eliminate background from neighboring masses. This has the effect of reducing the ion transmission at the desired m/z-value. In addition to this problem, electron impact detection of the propyl radical, C_3H_7, at m/z = 43 would be overwhelmed by background coming from dissociative ionization of propane, C_3H_8.

$$C_3H_8 \quad + \quad e^- \quad \rightarrow \quad C_3H_7^- \quad + \quad H \quad + \quad 2e^-$$

PI overcomes these problems. By tuning the undulator to 9.5 eV we were able to ionize the propyl radical (I.P. = 8.09 for n-propyl and 7.36 eV for iso-propyl radical) without significant ionization of propane (I.P. = 10.95 eV). This allowed us to lower the mass resolution of the quadrupole mass spectrometer to increase the ion transmission and instrument sensitivity.

Figure 10 shows a TOF spectrum of the propyl radical product of this reaction. The sources were rotated so that reactive products scattered 70° from the propane molecular beam entered the detector. The signal detected at m/z = 43 is due entirely to the propyl radical, appearing with a most probable arrival time $\tau_{mp} = 53$ μs and a minimum arrival time $\tau_{min} = 39$ μs. This corresponds to a most probable velocity, $\mathbf{v}_{mp} = 2200$ m/s and a maximum velocity $\mathbf{v}_{max} = 3000$ m/s.

This example of reactive scattering in a kinematically unfavorable reaction detecting alkyl radical reaction products in the presence of a large partial pressure of alkane parent together with the other examples of preliminary experiments makes a strong case that the new instrument does indeed surpass the abilities of previous machines based on EI.

4. *Acknowledgments*

This work was supported by the Director, Office of Energy Research, Office of Basic Energy Sciences, Chemical Sciences Division, of the U.S. Department of Energy under contract no. DE-AC03-76SF00098. We also appreciate the excellent jobs done on the beamline by the LBNL engineering staff, and all the support from the ALS staff.

5. Figure Captions

Figure 1. **Schematic Diagram of the Universal Crossed Molecular Beams Apparatus with Synchrotron Photo-ionization Mass Spectrometric Product Detection:** Two doubly differentially pumped molecular beam sources cross one another in the main chamber. The two molecular beam sources can be rotated about an axis normal to the plane of the page intersecting the beam crossing volume to allow different parts of the product angular distribution to be sampled by the detector. Scattered reaction products can enter the detector, which is a triply differentially pumped synchrotron photo-ionization quadrupole mass spectrometer. The photo-ionization volume is located 6 in. away from the molecular beams' crossing volume. A closed-cycle liquid Helium refrigerator cryo-pumps the photo-ionization region. Ionized reaction products are mass selected with a quadrupole mass filter and detected with a Daly Ion counter *(4)* consisting of a high voltage ion target producing secondary electrons which are detected with a scintillator/photomultiplier assembly. An electron-impact ionizer is also available. A slotted chopping wheel can be installed in front of the detector to allow for product velocity measurements through one of two ports. Some of the magnetically levitated turbo molecular pumps are shown (STP2000 etc. where the number indicates the pumping speed in ℓ/s)

Figure 2. **Three dimensional views of the dual rotating source assembly:** a) View of the roof of the source assembly. Two source chamber and one differential chamber pump-out ports on the "roof" are used with magnetically levitated turbo molecular pumps which can move when the source is rotated about its axis of near-cylindrical symmetry. A

port along the rotation axis of the source assembly can be used to cross a laser beam or the synchrotron beam with one or both of the molecular beams. A closed cycle liquid Helium refrigerator cools a Copper plate which is inserted through the port marked "background gobbler". See text. Access port for primary source is also shown. b) A view of the rotatable source from the interaction chamber. Access port for secondary source is shown. The differential pumping region for the secondary source is pumped through the port shown in this view. This circular port is also used together with a circular bearing and along with a circular bearing fitted to the very large circular surface on the source roof to allow for source rotation.

Figure 3. **Mechanical drawing showing another view of the rotating source assembly:** a) View of the source roof. (Shown in 3-D in fig. 2a). b) A cross-section through the roof shows the inner vacuum connections of the secondary source and differential pumping chambers. The laser access ports are also more clearly shown. The curved arrow shows how the second differential pumping chamber is evacuated through a fixed buffer chamber.

Figure 4. **Mechanical drawing of the main chamber:** The main chamber consists of the interaction chamber and the differential buffer chamber. a) A view of the main chamber along the rotation axis of the machine. b) A cross section of the main chamber. The 30" diameter circular surface holds the outer race of a mechanical bearing, the inner race of which holds the rotating source assembly. The same port holds three Carbon impregnated TEC-rings which seal the source and main chambers to one another. The 6" diameter port separating the Interaction chamber from the

buffer chamber seals the source against the main chamber with a single TEC-Ring. Narrow tubes located 4" 6" and 10" away from the centerline of the machine are used for introducing the synchrotron radiation. The port located 6" from the rotation axis has been used in all of the work described here.

Figure 5 **Three dimensional views of the main chamber:** a) One sees the main chamber from the side of the machine into which the VUV radiation enters. The large rectangular port orients the detector with respect to the crossing volume of the two molecular beams. The port used for installing the slotted chopping wheel can also be seen. The liquid nitrogen feed line delivers liquid nitrogen to large Copper panels which line the inside of the interaction chamber. The differential pump out port shows where the turbo molecular pump is attached to evacuate the buffer chamber. b) One sees the side of main chamber from which the rotating source assembly is inserted. The large circular port holds the rotating source assembly.

Figure 6. **Mechanical drawing of the differential pumping chamber assembly for the first two stages of the detector:** a) A view along the detection axis of the machine toward the molecular beam crossing volume. b) A cross-section of the detector chamber. Here one can see the way in which the synchrotron radiation is introduced and how access to the detector is achieved.

Figure 7. **Time-of-Flight (TOF) spectra of photodissociation products of Methylamine ($CH_3NH_2 \rightarrow CH_3 + NH_2$) at 193 nm:** The upper trace shows the TOF spectrum for the CH_3 radical detected at m/z = 15; the bottom trace results from the NH_2 radical,

detected at m/z = 16. There is no evidence of the much more likely H-atom loss channels because dissociative ionization of the CH_2NH_2 or CH_3NH radicals is suppressed by use of photo-ionization. Note that detection of reaction products at m/z = 15 and 16 is easily accomplished despite the large residual CH_4 background.

Figure 8. **Time-of-Flight (TOF) spectra of the photodissociation products of ozone ($O_3 \rightarrow O + O_2$) at 248 nm:** Upper trace shows the TOF spectrum of O-atoms detected at m/z = 16 and the lower trace shows the TOF spectrum of O_2 detected at m/z=32. Note the different time scales on the two TOF spectra. Note further the absence of O_2 peaks in the O-atom spectrum, clear evidence of the suppression of dissociative ionization of O_2. The peaks labeled 0,1,2,3,4 in the two TOF spectra are due to resolution of the individual vibrational states of $O_2(a^1\Delta)$.

Figure 9. **Time-of-Flight (TOF) spectra of the photodissociation products of Oxalyl chloride $(OCCl)_2$:** The upper trace shows the TOF spectrum of the CO photoproducts while the lower trace shows that of the Cl fragments. Note that the S/N ratio is comparable for the two experiments. Despite the large residual background of CO in the mass spectrometer, the use of cryogenic pumping in conjunction with VUV photo-ionization allows the reduction of CO background by 10^{2-3} in comparison to electron impact ionization.

Figure 10. **Newton Diagram of the $Cl + C_3H_8 \rightarrow HCl + C_3H_7$ crossed molecular beams experiment:** Laboratory frame vectors are indicated with "v's" while center-of-mass frame vector are indicated with "u's". $\mathbf{v}_{CM}$ is the velocity vector of the center-of-mass

of the system. The center-of-mass frame and laboratory frame are related by the vector equation $\mathbf{u} + \mathbf{v}_{CM} = \mathbf{v}$. The peak velocities of the Cl and C_3H_8 beams are labels $\mathbf{v}_{Cl}$ and $\mathbf{v}_{propane}$, respectively. A TOF spectrum (shown in figure 11) results from product detected along the direction of the vector, $\mathbf{v}_{mp}$. Products formed with the most probable velocity in the center-of-mass frame may be scattered anywhere on the circle touched by the tip of the vector $\mathbf{u}_{mp}$. Products formed with the maximum velocity in the center-of-mass frame may be scattered anywhere on the circle touched by the tip of the vector $\mathbf{u}_{max}$. Consequently, substantial product is detected at all accessible lab angles from -10 to 100°.. The collision energy of the reactants in the center-of-mass frame is 21 kcal/mol.

Figure 11. **TOF spectrum of the propyl radical from the reaction Cl + $C_3H_8 \rightarrow$ HCl + C_3H_7:** This common hydrocarbon free radical is detected with essential no background in a crossed molecular beams experiment whose Newton Diagram is shown in figure 10.

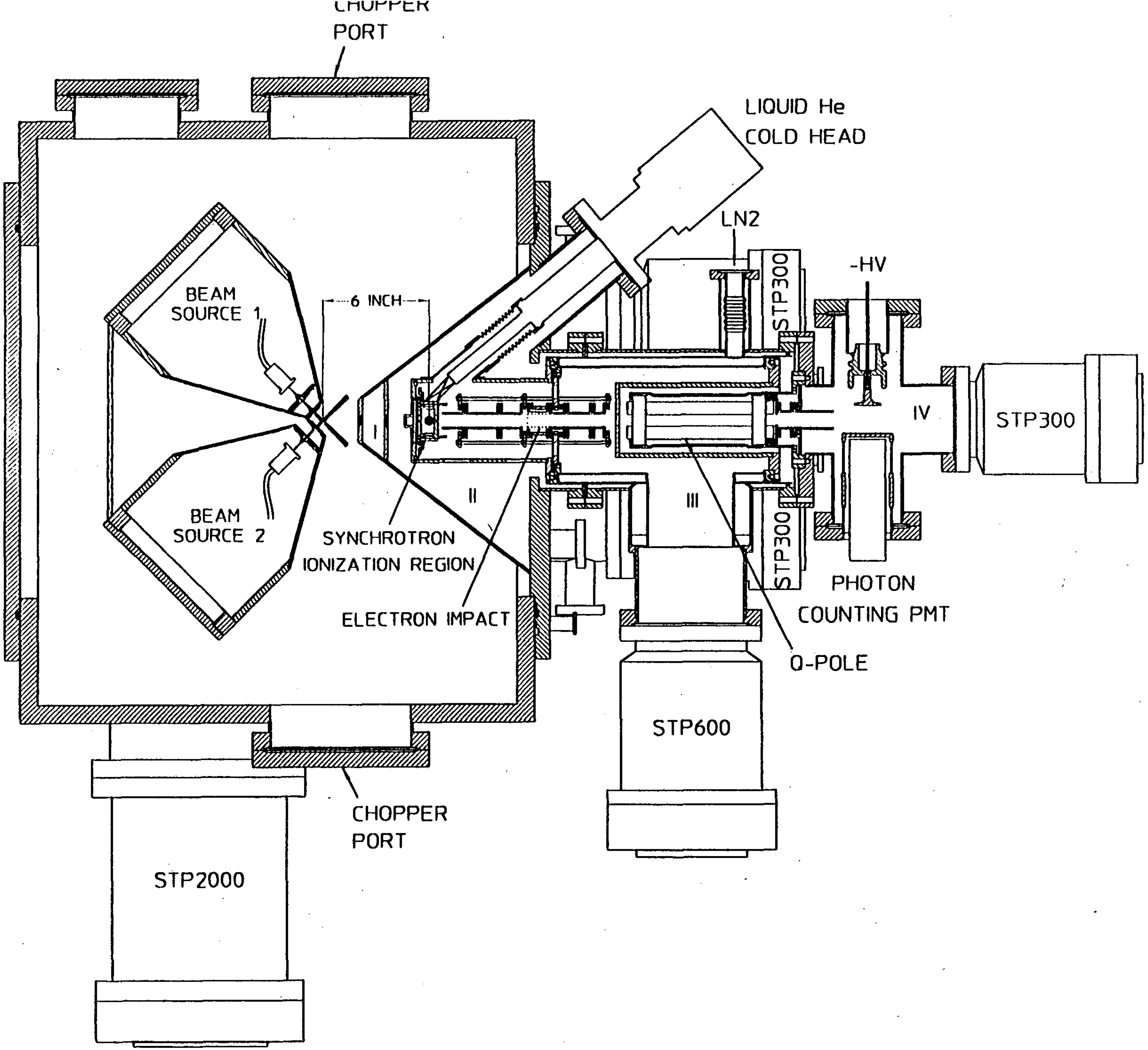
CHOPPER PORT
LIQUID He COLD HEAD
LN2
STP300
-HV
BEAM SOURCE 1
6 INCH
I
IV
STP300
BEAM SOURCE 2
II
III
STP300
SYNCHROTRON IONIZATION REGION
PHOTON COUNTING PMT
ELECTRON IMPACT
Q-POLE
STP600
CHOPPER PORT
STP2000

Figure 1

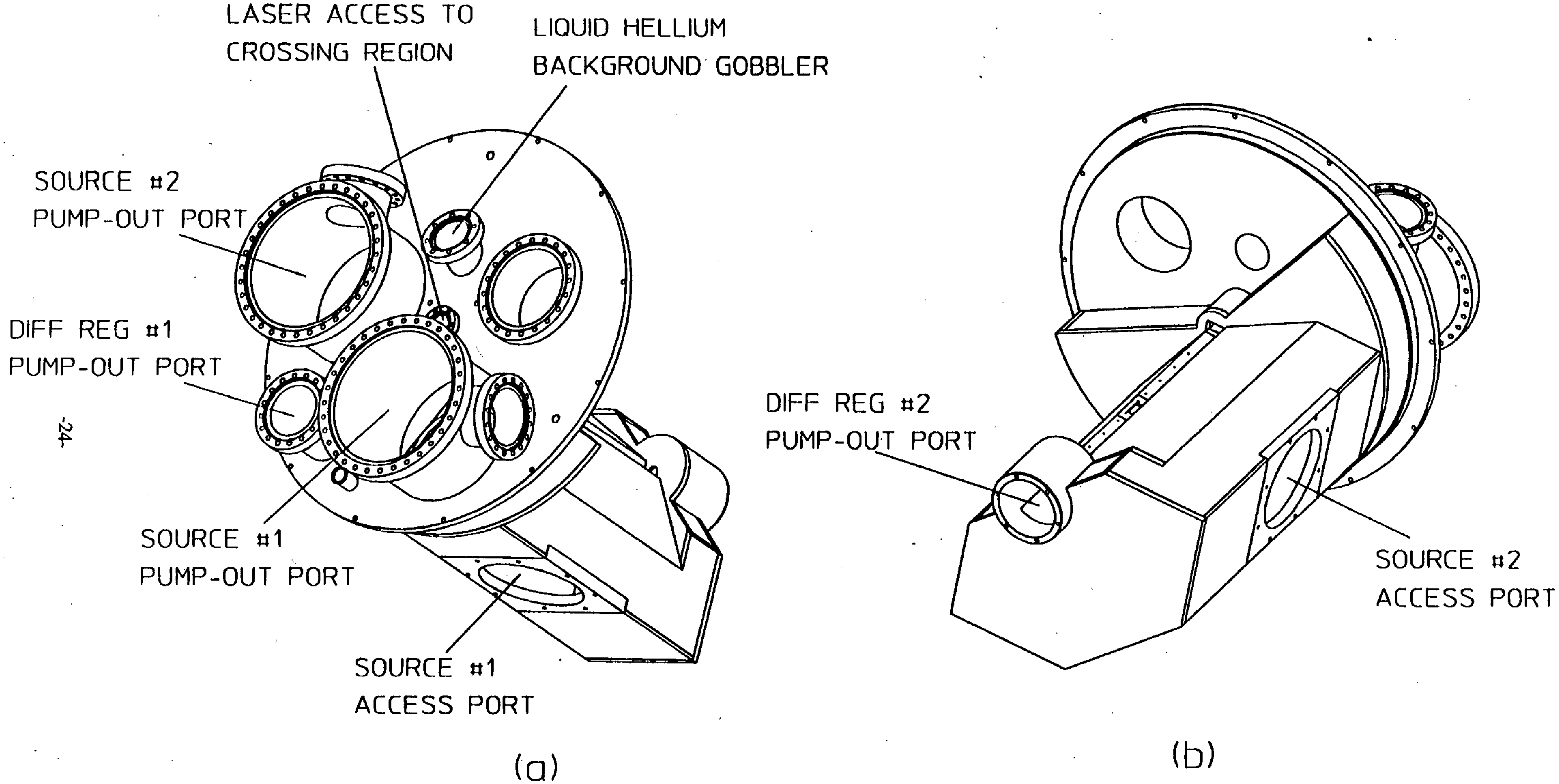
LASER ACCESS TO CROSSING REGION
LIQUID HELLIUM BACKGROUND GOBBLER
SOURCE #2 PUMP-OUT PORT
DIFF REG #1 PUMP-OUT PORT
SOURCE #1 PUMP-OUT PORT
SOURCE #1 ACCESS PORT
(a)
DIFF REG #2 PUMP-OUT PORT
SOURCE #2 ACCESS PORT
(b)

Figure 2

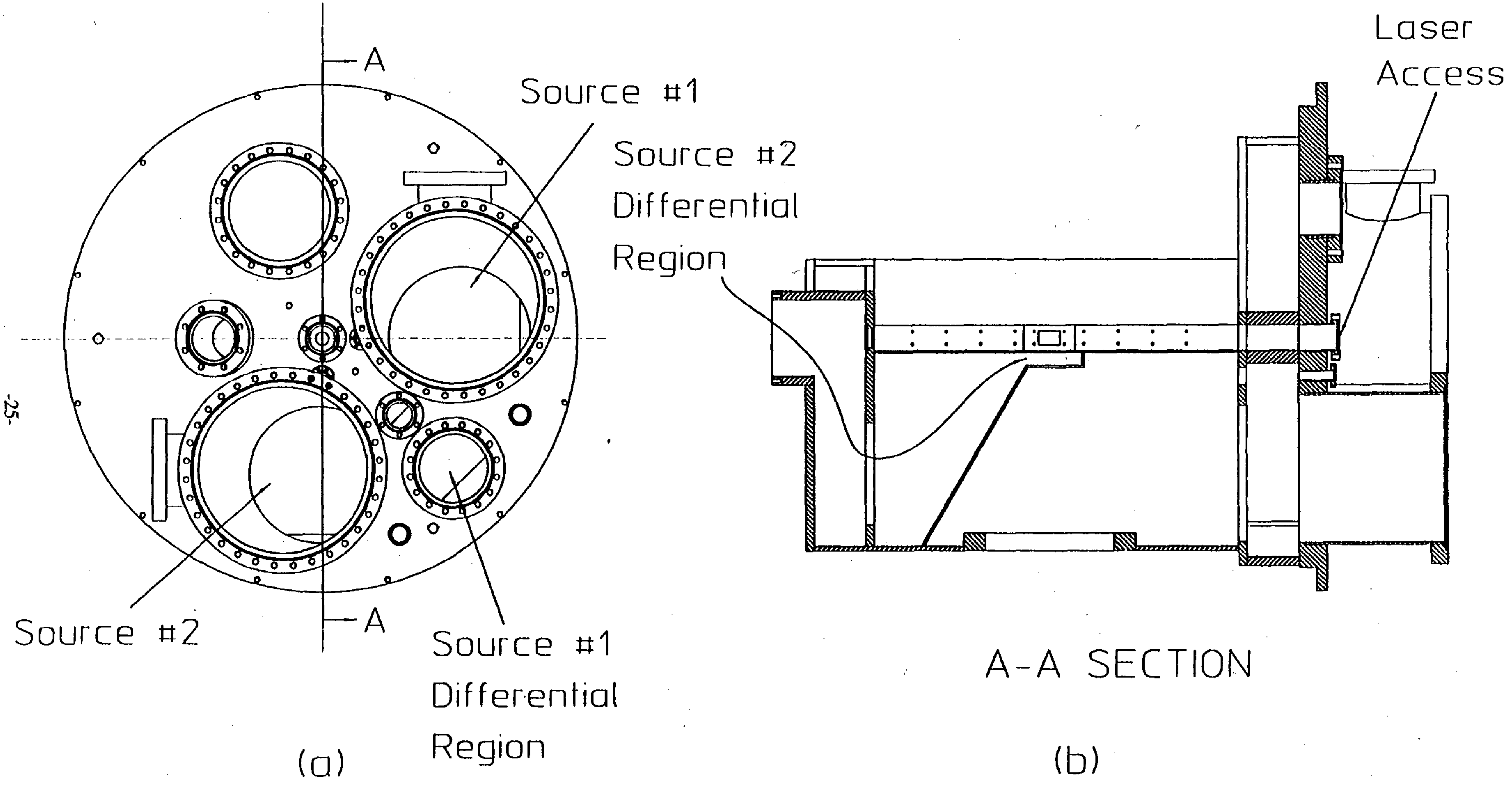
A
Source #1
Source #2
Differential
Region
Source #2
A
Source #1
Differential
Region
(a)
Laser
Access
A-A SECTION
(b)

Figure 3

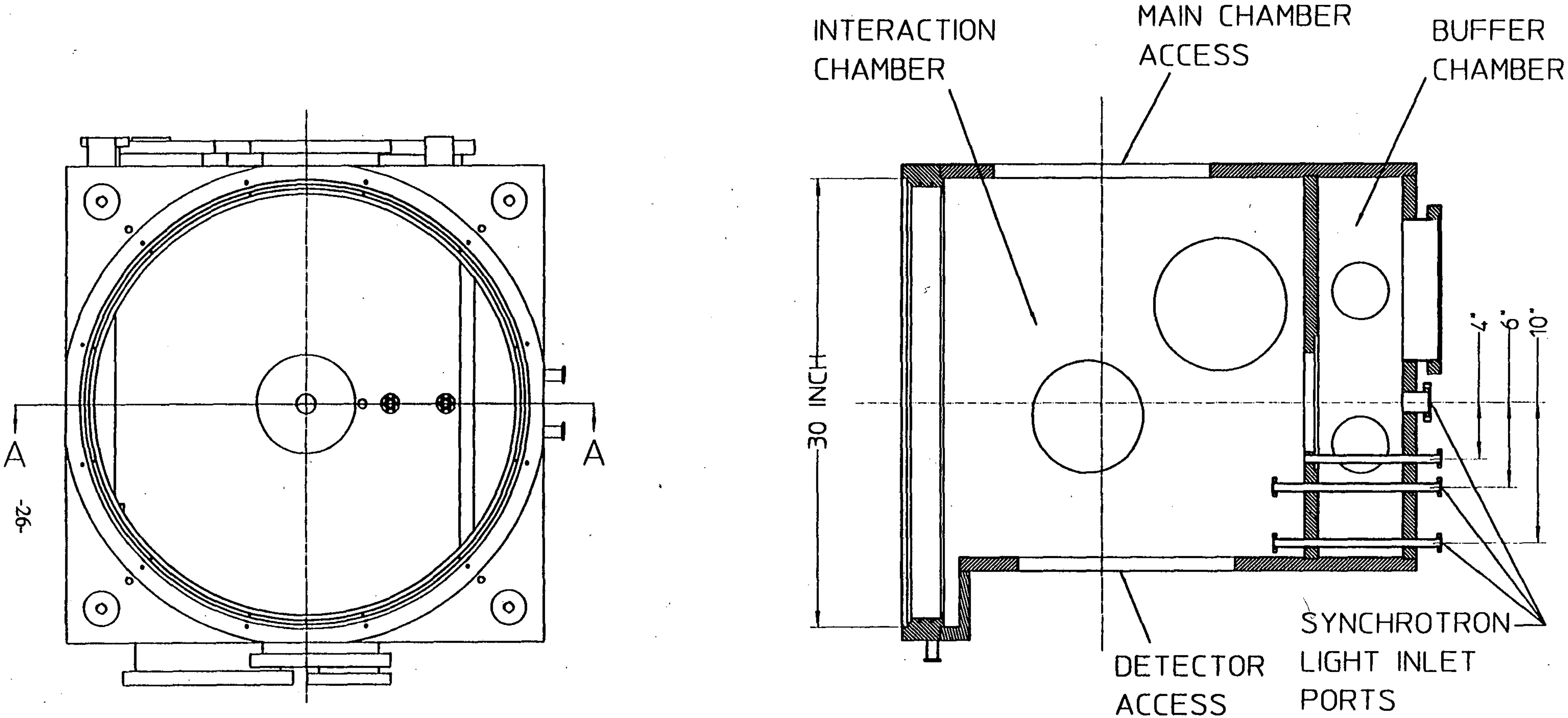

SECTION A-A

Figure 4

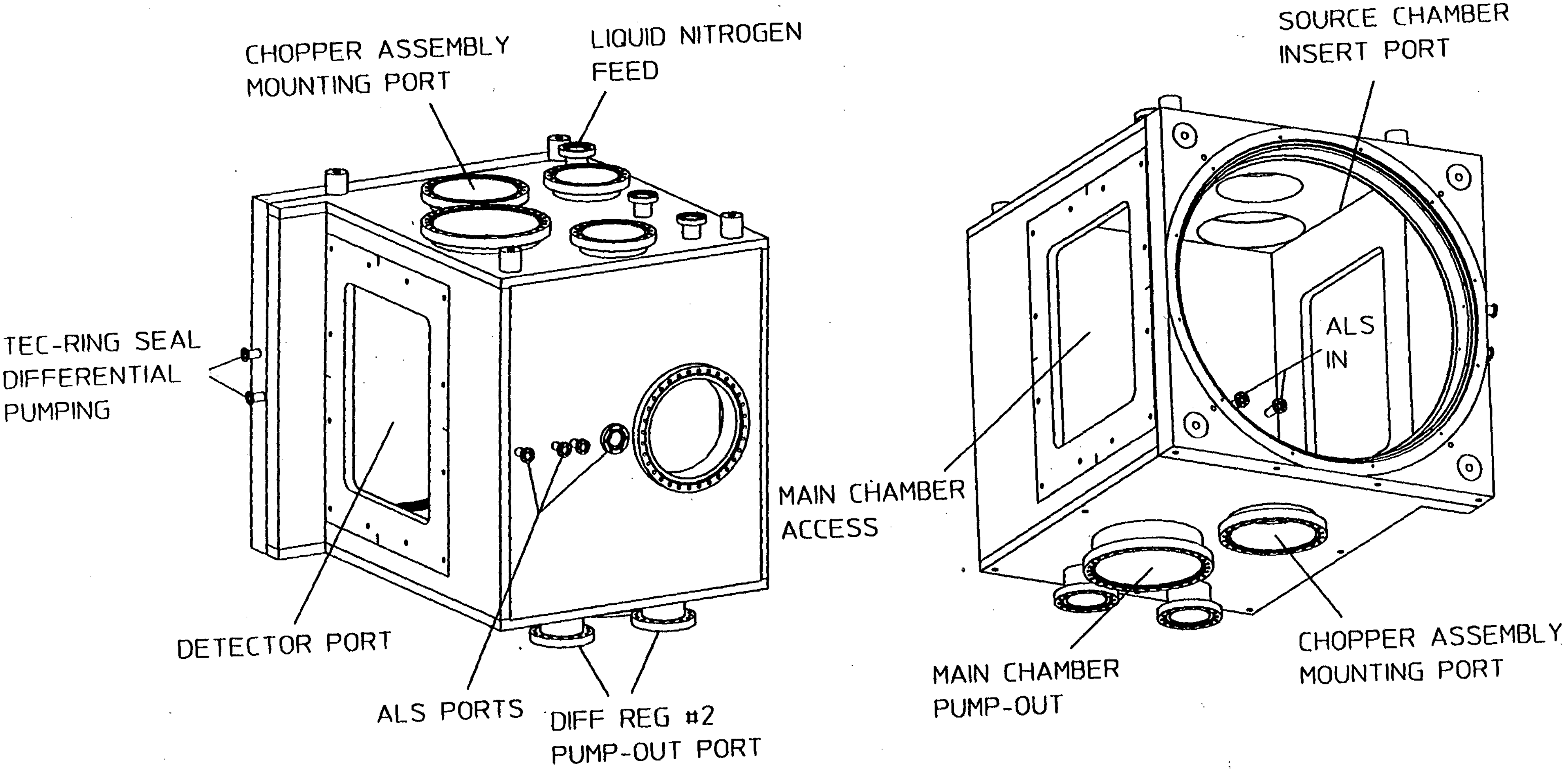
CHOPPER ASSEMBLY MOUNTING PORT
LIQUID NITROGEN FEED
TEC-RING SEAL DIFFERENTIAL PUMPING
DETECTOR PORT
ALS PORTS
DIFF REG #2 PUMP-OUT PORT
MAIN CHAMBER ACCESS
SOURCE CHAMBER INSERT PORT
ALS IN
MAIN CHAMBER PUMP-OUT
CHOPPER ASSEMBLY MOUNTING PORT

Figure 5

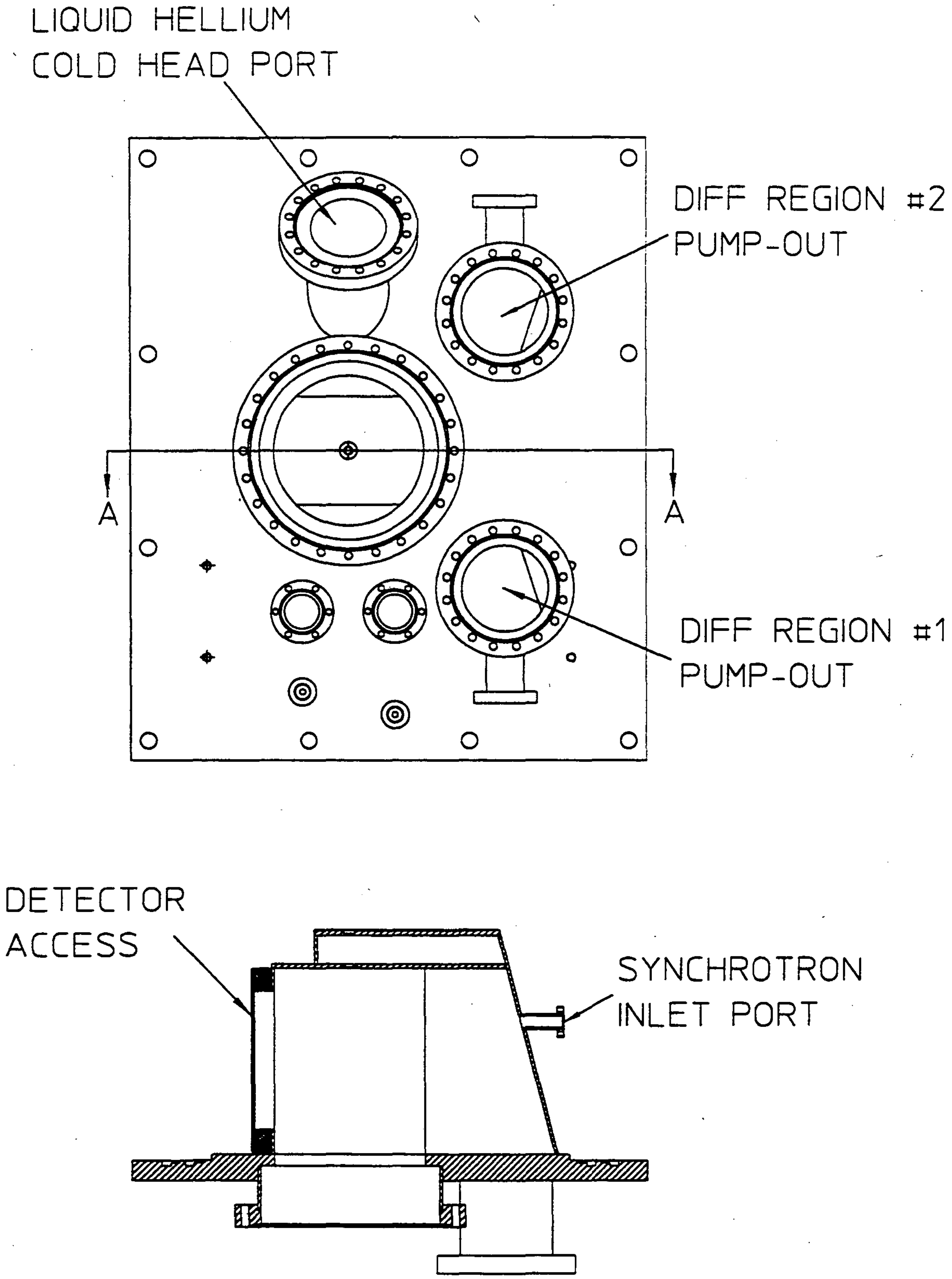

B-B SECTION

Figure 6

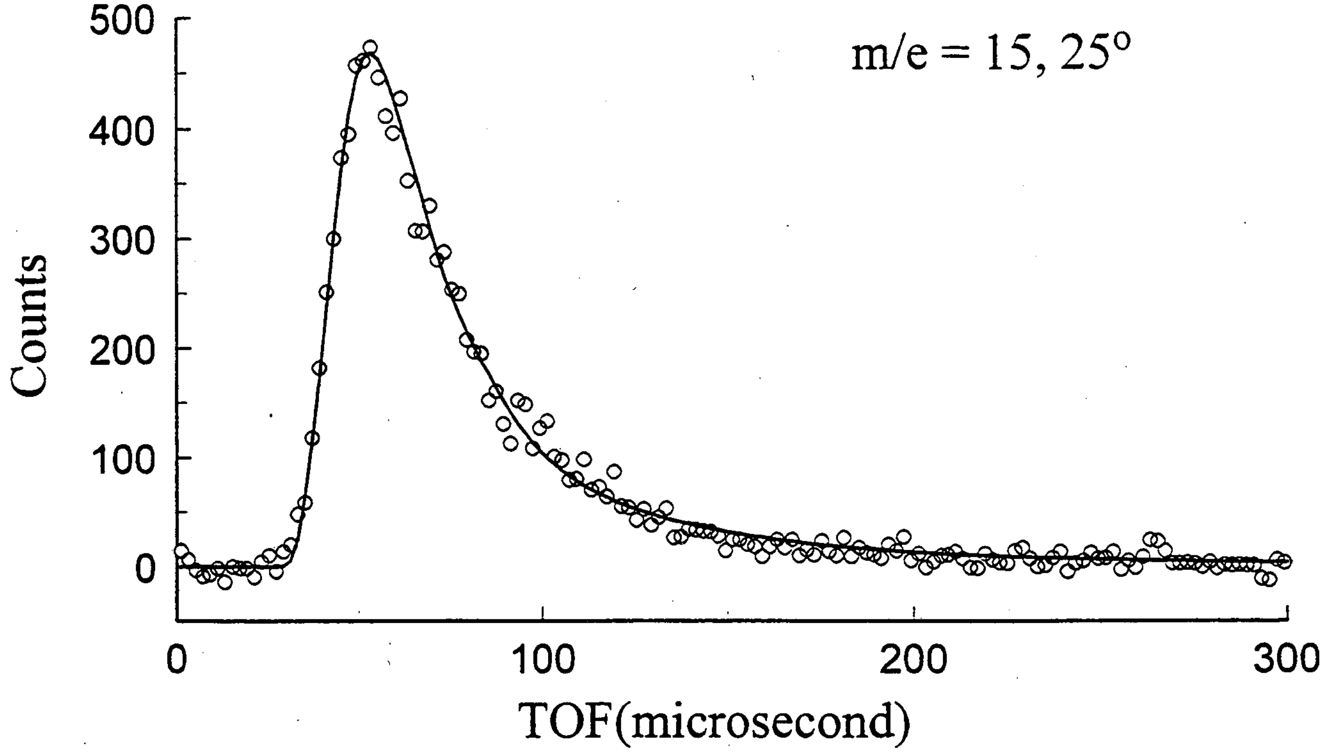
m/e = 15, 25°
Counts
500
400
300
200
100
0
0
100
200
300
TOF(microsecond)

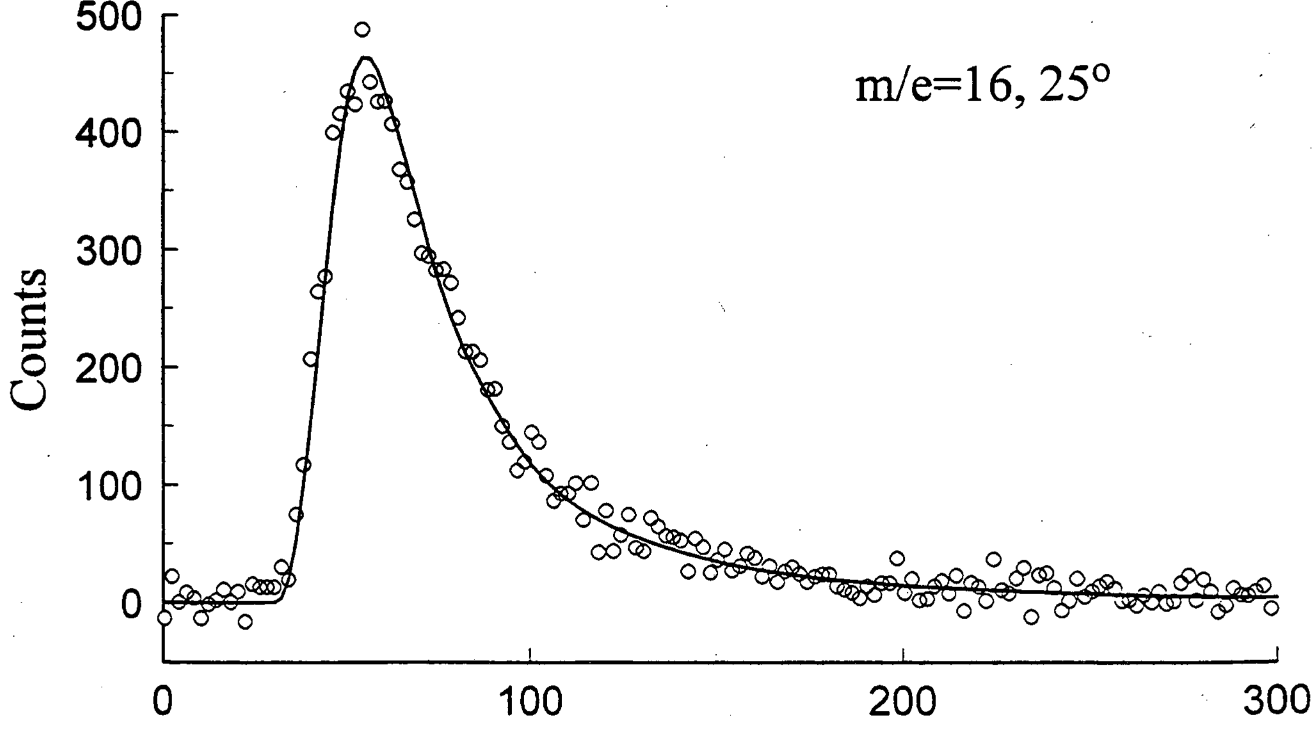
m/e=16, 25°
Counts
500
400
300
200
100
0
0
100
200
300
TOF(microsecond)

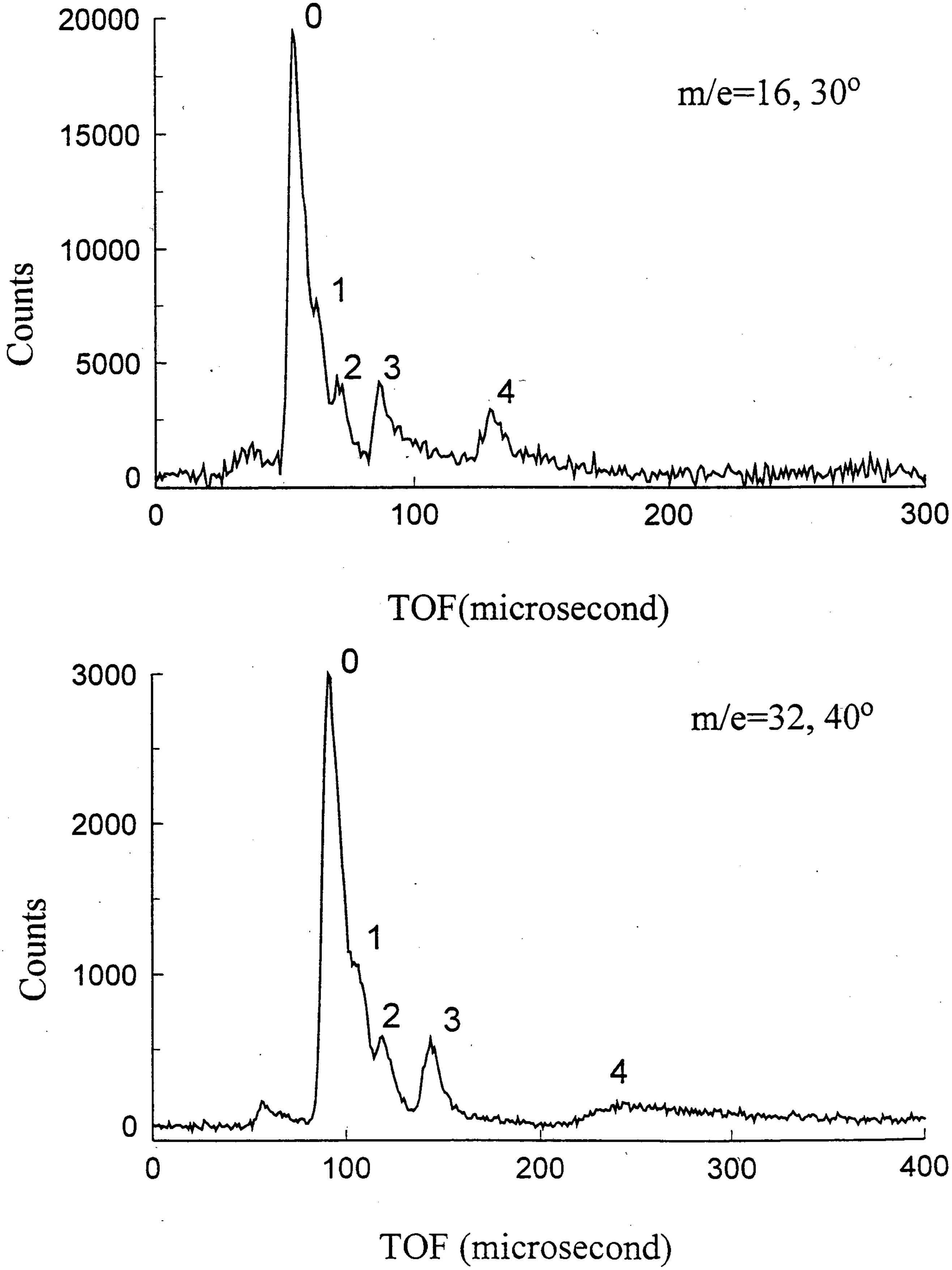
20000
15000
10000
5000
0
Counts
0
1
2
3
4
m/e=16, 30°
0
100
200
300
TOF(microsecond)
3000
2000
1000
0
Counts
0
1
2
3
4
m/e=32, 40°
0
100
200
300
400
TOF (microsecond)

Figure 8

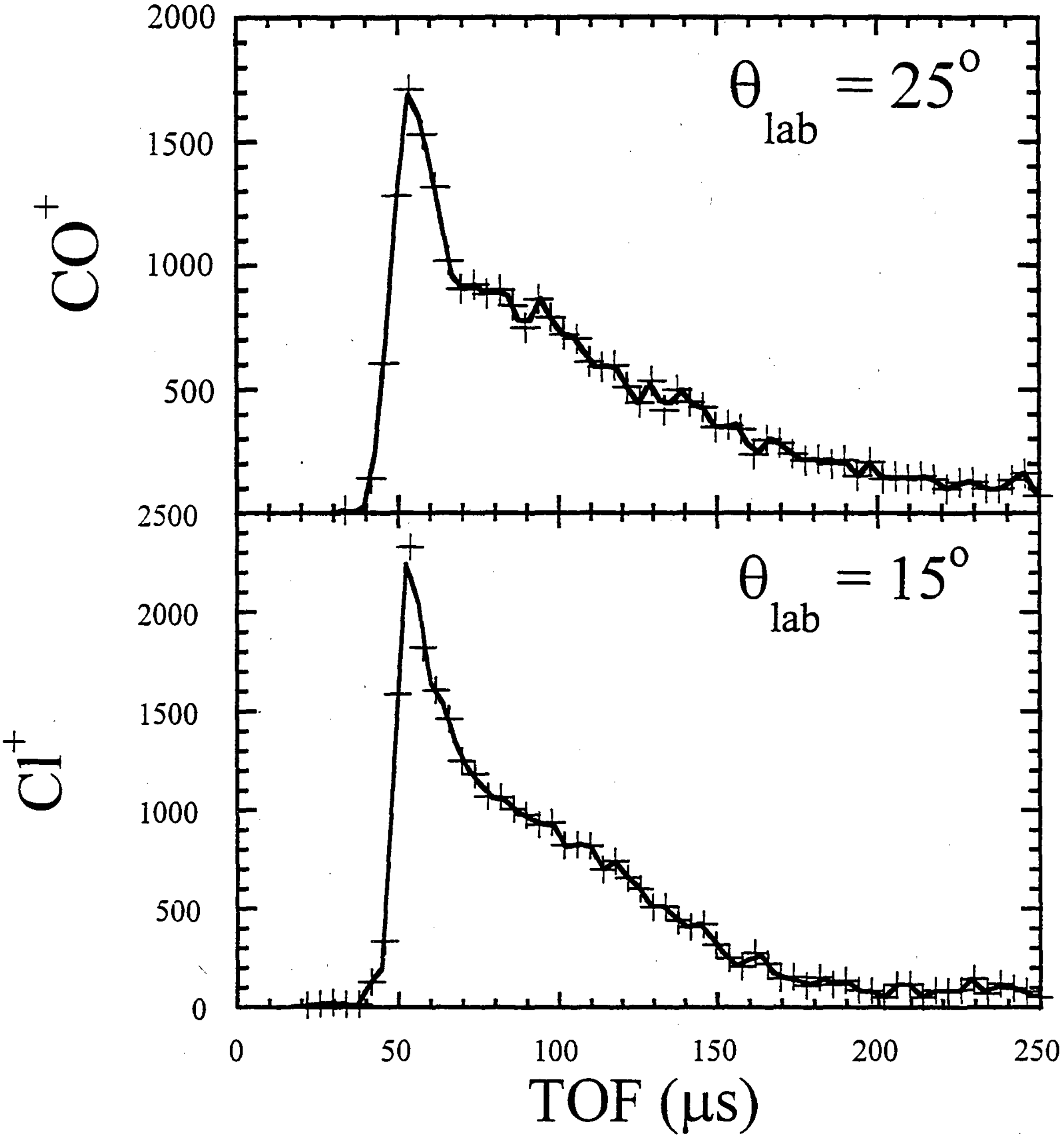
2000
1500
1000
500
2500
2000
1500
1000
500
0
CO^+
Cl^+
$\theta_{lab} = 25°$
$\theta_{lab} = 15°$
0
50
100
150
200
250
TOF (μs)

Figure 9

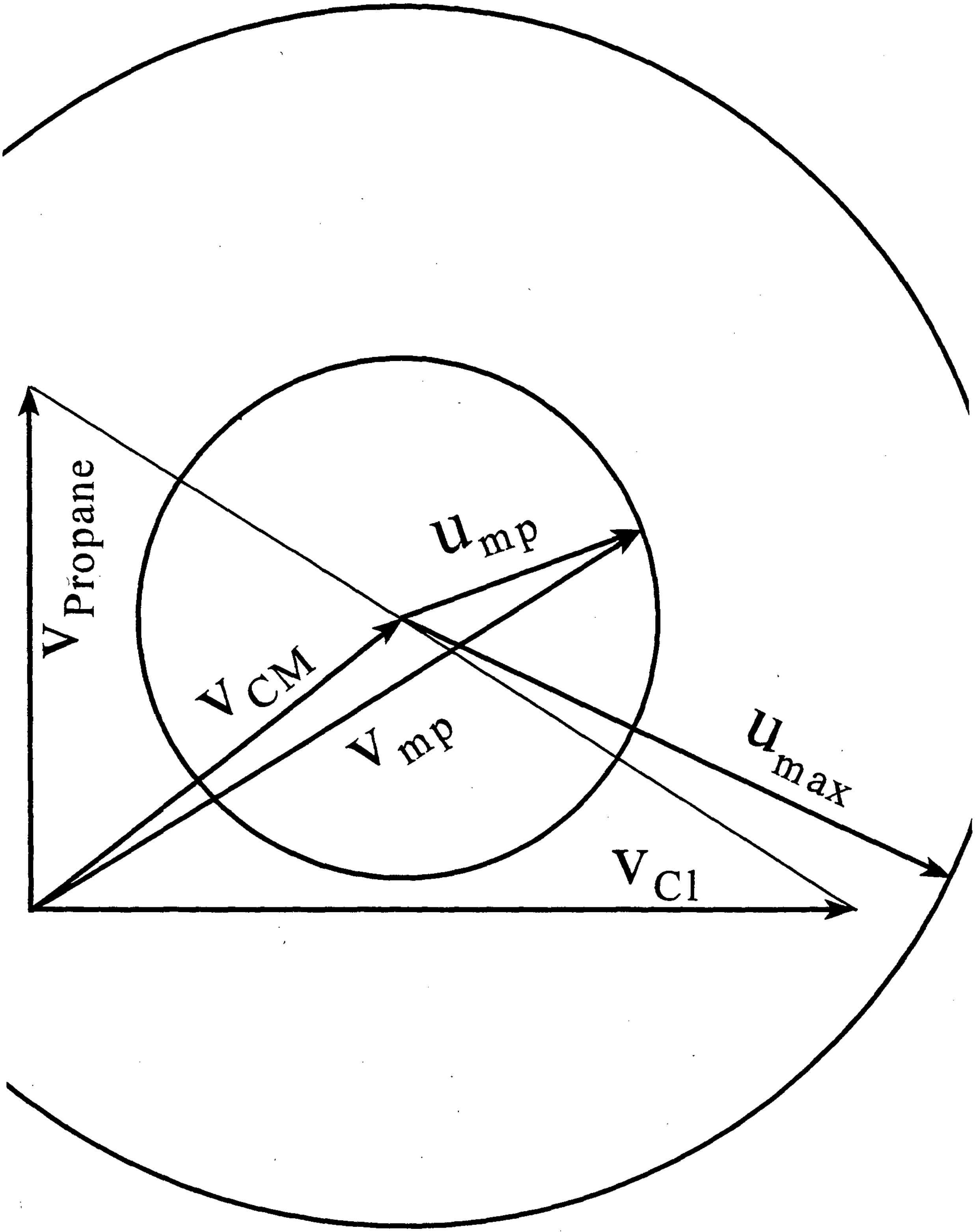

Figure 10

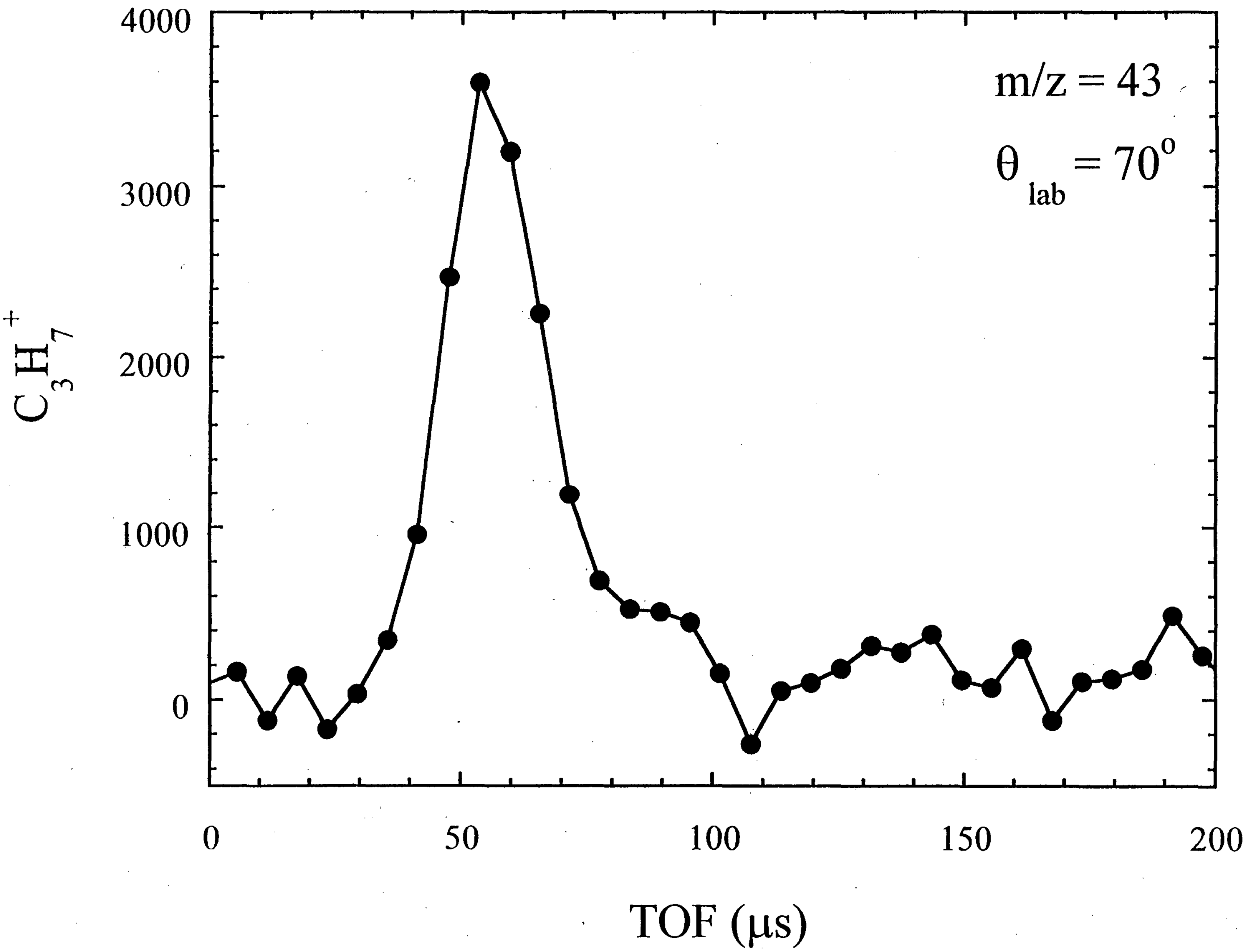
4000
3000
2000
1000
0
$C_3H_7^+$
0
50
100
150
200
TOF (μs)
m/z = 43
$\theta_{lab} = 70^o$

Figure 11

6. References

1. Y. T. Lee, J. D. McDonald, P. R. LeBreton and D. R. Herschbach, *Rev. Sci. Instrum.* **40**, 1402 (1969)

2. Y. T. Lee, *Science* **236**, 793 (1987)

3. A. M. Wodtke and Y. T. Lee, *J. Phys. Chem.* **89**, 4744 (1985)

4. N. R. Daly, *Rev. Sci. Intrum.* **31**, 264 (1960)

5. Lawerence Berkeley National Laboratory and the University of California, 1-2 GeV Synchrotron Radiation Source (1986).

6. X. Yang, D. A. Blank, J. Lin, P. A. Heimann, A. M. Wodtke, Y. T. Lee and A. G. Suits, in *Synchrotron Radiation techniques in Industrial Chemical and Material Science* D'Amico, Eds. (Plenum Press, New York, 1996).

7. P. A. Heimann, M. Koike, C. W. Hsu, M. Evans, C. Y. Ng, D. A. Blank, A. G. Suits and Y. T. Lee, SPIE, (1996), vol. 2856, pp. 90.

8. A. G. Suits, P. Heimann, X. Yang, M. Evans, C. W. Hsu, K. Lu, A. H. Kung and Y. T. Lee, *Rev. Sci. Instrum.* **66**, 5405 (1995)

9. G. C. G. Waschewsky, D. C. Kitchen, P. W. Browning and L. J. Butler, *J. Phys. Chem.* **99**, 2635 (1995)

10. D. Stranges, X. Yang, J. D. Chesko and A. G. Suits, *J. Chem. Phys.* **102**, 6067 (1995)

11. R. K. Sparks, L. R. Carlson, K. Shobatake, M. L. Kowalczyk and Y. T. Lee, *J. Chem. Phys.* **72**, 1401 (1980)

12. M. Ahmed and A. G. Suits, 212th ACS National Meeting, Orlando, FL, (1996),

ERNEST ORLANDO LAWRENCE BERKELEY NATIONAL LABORATORY
ONE CYCLOTRON ROAD | BERKELEY, CALIFORNIA 94720

Prepared for the U.S. Department of Energy under Contract No. DE-AC03-76SF00098